A simulation study of linker vacancy distribution and its effect on UiO-66 stability

Esteban Acuna-Yeomans [a], J. J. Gutiérrez-Sevillano [b,*], David Dubbeldam [c], Sofia Calero [a,*]

[a] Materials Simulation and Modelling, Department of Applied Physics and Science Education, Eindhoven University of Technology, 5600 MB Eindhoven, The Netherlands

[b] Department of Physical, Chemical and Natural Systems, Universidad Pablo de Olavide, Ctra. Utrera Km. 1, Seville ES-41013,

[c] Van 't Hoff Institute for Molecular Sciences, University of Amsterdam, Science Park 904, 1098XH Amsterdam, The Netherlands

Supporting Information

Atom nomenclature and force field parameters

The tables included in this subsection contain the interaction parameters for each term of the Universal Force Field[S1], as used in this work. The atom types referenced in the text and tables are labelled according to the pictured nomenclature (Figure S1).

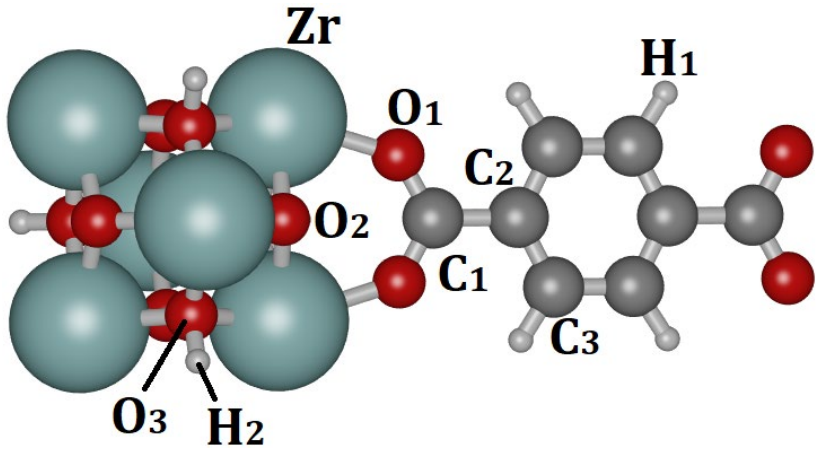

Figure S1: Atom nomenclature used in this work.

The parameters were initially calculated using the 'LAMMPS interface' python module created by P. Boyd, M. Moosavi and M. Witman for the publication by Boyd et al.[S2]. The module takes a crystallographic information file (CIF) as input to generate the parameter sets. In this work, we

used the pristine UiO-66 CIF constructed by D. Dubbeldam included in the RASPA2 simulation package[S3] based on previously reported experimental measurements by J.S. Cavka et al.[S4]. The derivation of the outputted parameters were verified according to the UFF recipes, reformatted according to our atom nomenclature and used in the creation of the LAMMPS input files.

$$U_{\text{bonds}} = \frac{1}{2}K_r(r - r_0)^2$$

Bond	K_r [kcal/(mol·Å²)]	r_0[Å]
C3-C3	925.31	1.379
C3-C2	925.31	1.379
C3-H1	714.88	1.081
C1-O1	1293.36	1.312
C1-C2	783.34	1.458
O3-H2	1119.99	0.990
O1-Zr	582.00	2.127
O3-Zr	598.89	2.107
O2-Zr	618.00	2.085

Table S1: Parameters for the bond stretching potential energy contribution of the force field.

$$U_{\text{angles}} = \frac{K_\theta}{n^2}[1 - \cos(n\theta)]$$

Bend	K_θ [kcal/mol]	n
C3-C3-C2	111.30	3
C3-C2-C3	111.30	3
C3-C3-H1	57.29	3
C2-C3-H1	57.29	3
O1-C1-O1	187.14	3
C2-C1-O1	131.76	3
C3-C2-C1	102.18	3
C1-O1-Zr	124.83	3
Zr-O2-Zr	118.51	3

$$U'_{\text{angles}} = K_\theta[C_0 + C_1\cos(\theta) + C_2\cos(2\theta)]$$

Bend	K_θ [kcal/mol]	C_0	C_1	C_2
Zr-O3-Zr	331.86	0.300	0.267	0.267
H2-O3-Zr	122.14	0.300	0.267	0.267
O3-Zr-O2	116.83	0.344	0.375	0.281
O1-Zr-O2	115.14	0.344	0.375	0.281
O1-Zr-O2	115.14	0.344	0.375	0.281
O1-Zr-O3	113.38	0.344	0.375	0.281
O1-Zr-O3	113.38	0.344	0.375	0.281
O1-Zr-O1	111.77	0.344	0.375	0.281
O1-Zr-O1	111.77	0.344	0.375	0.281
O2-Zr-O2	118.69	0.344	0.375	0.281
O3-Zr-O3	115.02	0.344	0.375	0.281

Tables S2 and S3: Parameters for the angle bending contributions of the force field. The coefficients C0, C1 and C2 are derived according to the recipe provided in the original article [ref] given an equilibrium angle. The specific coefficients used in this work were obtained using the equilibrium angle generated by the 'LAMMPS interface' python module[2].

$U_{\text{dihedrals}} = \frac{K_\varphi}{2}\left[1 - \cos\left(m\varphi_0\right)\cos(m\varphi)\right]$		
Dihedral	**K_φ [kcal/mol]**	**m**
H1-C3-C2-C1	6.74	2
H1-C3-C2-C3	6.74	2
H1-C3-C3-H1	6.74	2
H1-C3-C3-C2	6.74	2
C3-C3-C2-C3	6.74	2
C3-C3-C2-C1	6.74	2
C2-C3-C3-C2	6.74	2
C2-C1-O1-Zr	13.47	2
O1-C1-O1-Zr	13.47	2
O1-C1-C2-C3	2.50	2

Table S4: Parameters for the dihedral torsion potential. UFF stipulates there should be no dihedrals defined for metal ions in the two middle positions. The equilibrium angle φ_0 for the defined dihedrals is either 0 or π.

$U_{\text{impropers}} = K_\xi[C_0 + C_1\cos(\xi) + C_2\cos(2\xi)]$				
Improper	**K_ξ [kcal/mol]**	**C_0**	**C_1**	**C_2**
C3-C3-C2-H1	2	1	-1	0
C3-H1-C3-C2	2	1	-1	0
C3-C2-H1-C3	2	1	-1	0
C1-C2-O1-O1	2	1	-1	0
C1-O1-C2-O1	2	1	-1	0
C1-O1-O1-C2	2	1	-1	0
C2-C3-C3-C1	2	1	-1	0
C2-C1-C3-C3	2	1	-1	0
C2-C3-C1-C3	2	1	-1	0
O2-Zr-Zr-Zr	2	1	-1	0

Table S5: Parameters for the bond stretching term of the force field. The coefficients C0, C1 and C2 were taken directly from the original UFF publication.

$U_{\text{LJ}} = 4\epsilon\left[\left(\frac{\sigma}{r_{ij}}\right)^{12} - \left(\frac{\sigma}{r_{ij}}\right)^{6}\right]$		
Atoms	**ϵ [kcal/mol]**	**σ [Å]**
Zr - Zr	0.069	2.783
O1 - O1	0.060	3.118
O2 - O2	0.060	3.118
O3 - O3	0.060	3.118
C1 - C1	0.105	3.431
C2 - C2	0.105	3.431
C3 - C3	0.105	3.431
H1 - H1	0.044	2.571
H2 - H2	0.044	2.571

Table S6: Non-bonded interaction parameters for the Lennard-Jones potential. Taken directly from the original UFF publication[S1].

Comparison with alternative reference set

In the main text a comparison with a reference set of 8 structures is presented. Said structures were created sequentially by introducing linker vacancies in an orderly fashion to the pristine UiO-66 structure (see Fig. 4). In order to determine the degree to which the vacancy introduction process impacts the result, we generated an alternative reference set in which the same vacancies are introduced randomly. As can be seen in figures S1 and S2, the amorphization pressures for every pair of structures with N vacancies is similar. The extrapolated values for 0 linker vacancies are quite similar as well.

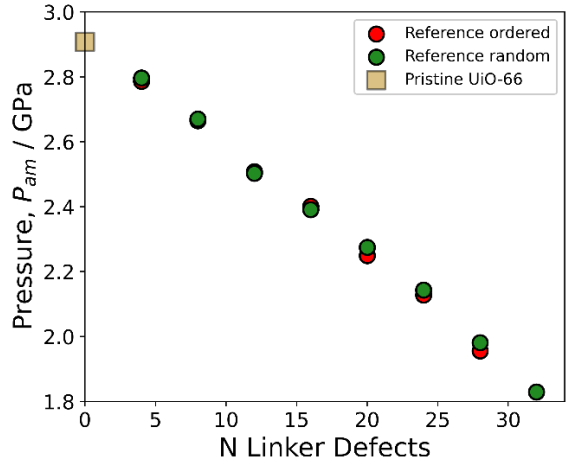

Figure S2: Amorphization pressure with respect to the number of linker vacancies for the reference systems. The red data points correspond to structures in which the vacancies were introduced in order and the green data points correspond to structures where the same defects were introduced randomly. The extrapolated N=0 values for the ordered and random reference systems are 2.934GPa and 2.935GPa, respectively.

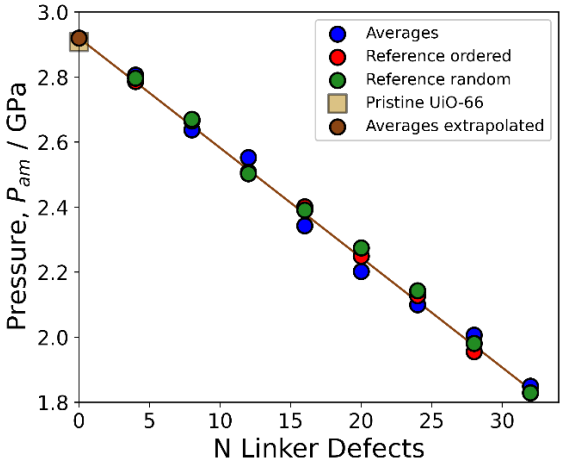

Figure S3: Comparison between the reference systems (red and green) and the average amorphization pressure value for each set of defected structures (blue circles). The line represents the linear extrapolation of the average values. The extrapolated Pam estimation for a structure with 0 linker defects is 2.92GPa which is close to the amorphization pressure of the pristine structure obtained using MD (2.908GPa).

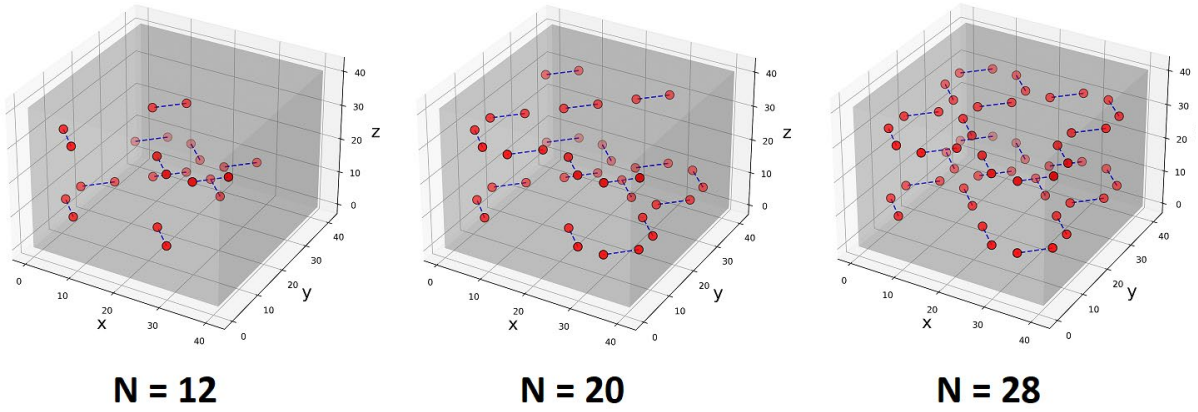

Figure S4: Pictorial representation of the structures with 12, 20 and 28 randomly introduced linker vacancies. The vacancies are the same ones as those previously introduced in an orderly fashion and used as a reference in the main text, therefore the N = 32 structure is the same for both sets.

Amorphization pressure w/r/t number of linker vacancies

As mentioned in the main text, for each defective structure certain distance-based metrics were calculated. Figures S4 and S5 are Pam v.s N plots where the data for each structure is coloured according to the mean distance between vacancies and the mean distance w/r/t the geometric centre of the supercell, respectively.

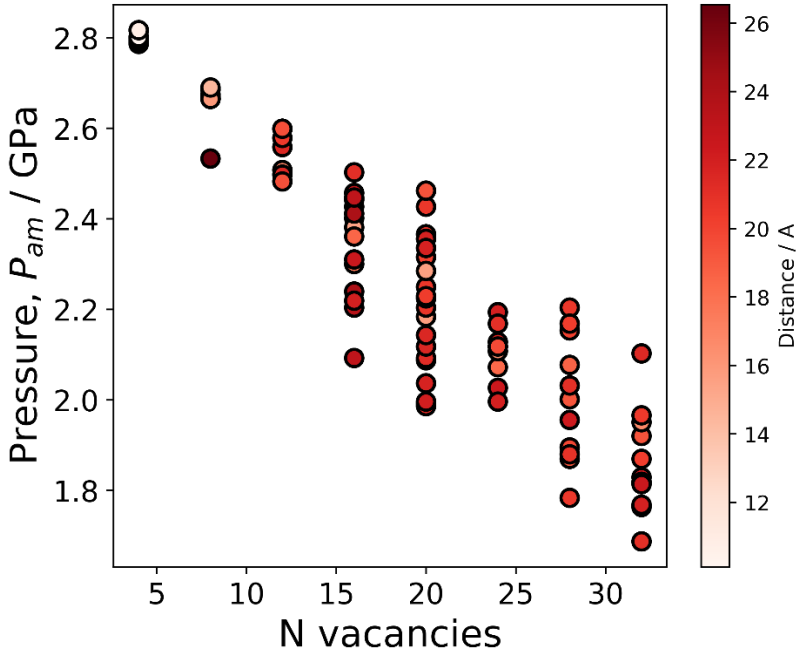

Figure S5: Amorphization pressure with respect to the number of linker vacancies contained for all defected structures of study. Each data point corresponds to a defected structure with different vacancy spatial concentration, orientation and order. The data points are colored according to the mean distance between linker vacancies (in Angstroms). As can be seen in the picture, this metric cease to be a good differentiator of structures with more than a few linker vacancies.

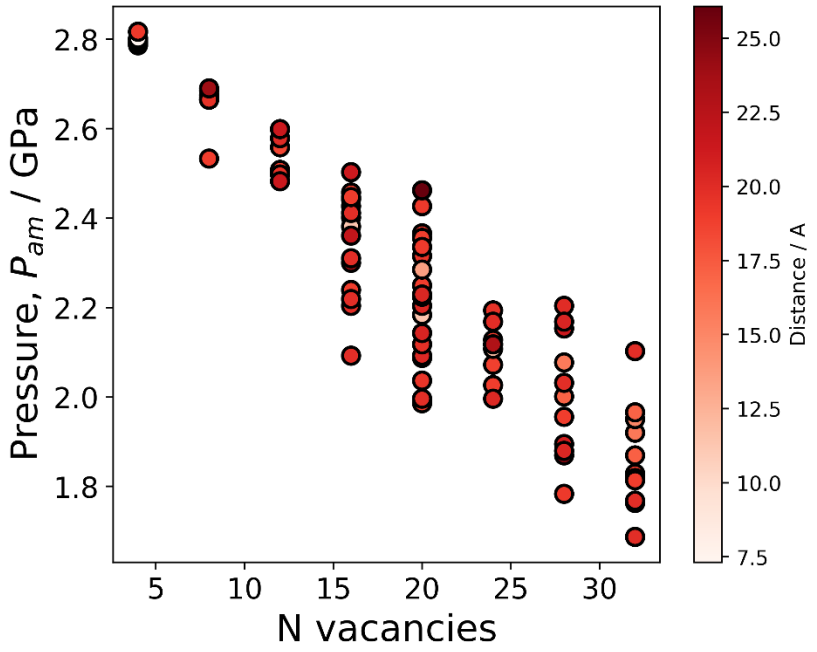

Figure S6: Amorphization pressure with respect to the number of linker vacancies contained for all defected structures of study. Each data point corresponds to a defected structure with different vacancy spatial concentration, orientation and order. The data points are colored according to the mean distance from linker vacancies to the geometric center of the supercell (in Angstroms).

Orientation of BDC linkers in UiO-66

Each defected structure was also characterized according to the number missing linkers that had a particular orientation. In UiO-66 we can find 6 distinct BDC linker orientations. Figure S6 shows the orientation type nomenclature used in this work.

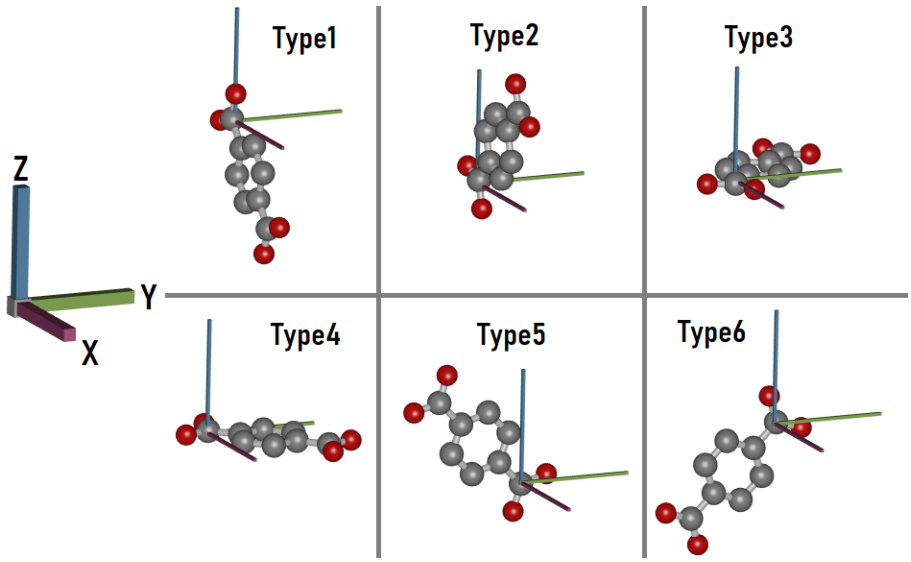

Figure S7: BDC linker orientation nomenclature used in this work. Orientation type is categorized according to their position with respect to cartesian coordinate axes.

Results for structures with 20 linker vacancies

Structures with 20 defects											
Pam [GPa]	**Dv [A]**	**Dc [A]**	**N Type1**	**N Type2**	**N Type3**	**N Type4**	**N Type5**	**N Type6**	**Kv [GPa]**	**Eani [GPa]**	**Bani [GPa]**
1.986	21.43	18.90	20	0	0	0	0	0	50.22	3.36	9.99
1.991	21.46	19.05	0	0	0	0	20	0	50.21	3.38	10.34
1.996	22.07	19.80	0	0	2	16	0	2	48.04	3.02	7.98
2.037	21.80	19.45	2	1	0	16	1	0	47.56	3.04	6.22
2.087	21.21	19.98	0	0	20	0	0	0	50.52	3.10	7.17
2.092	21.27	20.32	0	20	0	0	0	0	50.30	3.26	8.79
2.118	21.58	19.70	0	0	0	20	0	0	50.12	3.26	8.70
2.143	21.54	20.51	0	0	0	0	0	20	50.45	3.06	6.78
2.184	15.70	11.34	5	4	3	2	5	1	45.12	1.38	1.65
2.204	20.74	20.37	10	0	10	0	0	0	47.80	1.94	3.42
2.224	20.84	19.93	0	0	0	10	0	10	48.03	1.92	3.28
2.229	20.37	20.39	5	0	5	5	0	5	46.10	1.49	1.76
2.285	15.58	13.60	4	4	4	2	3	3	46.06	1.25	1.24
2.315	20.09	19.49	3	2	2	7	3	3	46.72	1.40	1.53
2.336	21.91	19.06	0	2	1	0	0	17	50.66	2.04	2.72
2.356	21.85	18.87	0	1	1	1	1	16	50.60	1.79	2.11
2.366	20.76	19.35	3	2	4	3	4	4	47.04	1.21	1.13
2.427	20.58	19.18	3	3	3	3	4	4	47.46	1.23	1.11
2.462	19.31	26.07	3	1	6	3	4	3	50.40	1.26	1.21

Table S7: Comparison of amorphization pressure (Pam), mean distance between vacancies (Dv), mean distance to the center of the supercell (Dc), number of linkers according to orientation type, bulk modulus and anisotropies for the structures containing 20 defects studied in this work. Data is ordered according to amorphization pressure, in ascending order.

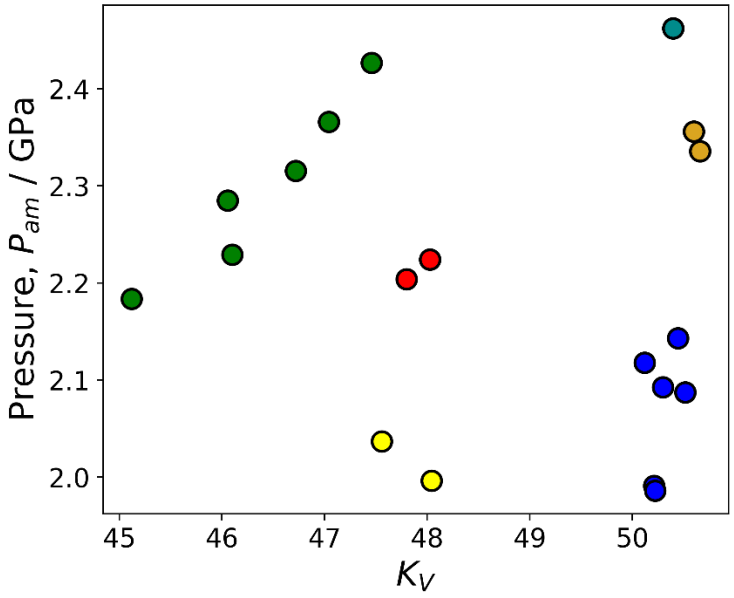

Figure S8: Amorphization pressure v.s bulk modulus plot for the 19 structures containing 20 linker vacancies studied in this work. The data points are colored according to the following: (1) green circles correspond to structures where the vacancies were selected randomly from the whole volume, (2) teal circles to structures where the vacancies were selected quasi-randomly from an outer sub-volume, (3) blue circles to structures where all missing linkers had the same orientation (1 point per orientation type), (4) yellow circles correspond to structures where 16 of the 20 missing linkers had type4 orientation and the rest were selected randomly, (5) gold circles correspond to structures where 16 of the 20 missing linkers had type6 orientation and the rest were selected randomly, (6) red circles correspond to structures where 10 missing linkers had one type of orientation and 10 missing linkers had another.

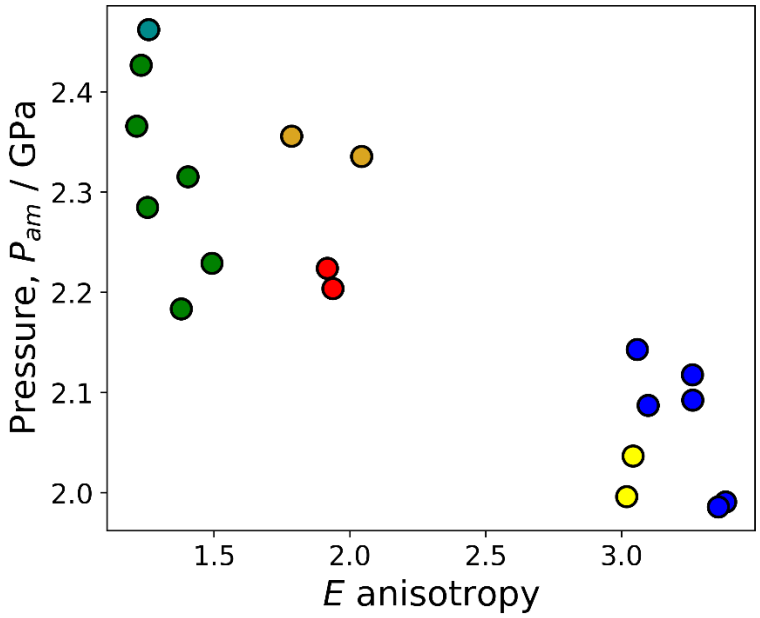

Figure S9: Amorphization pressure v.s young modulus anisotropy plot for the 19 structures containing 20 linker vacancies studied in this work. The data points are colored as indicated in Fig. S7

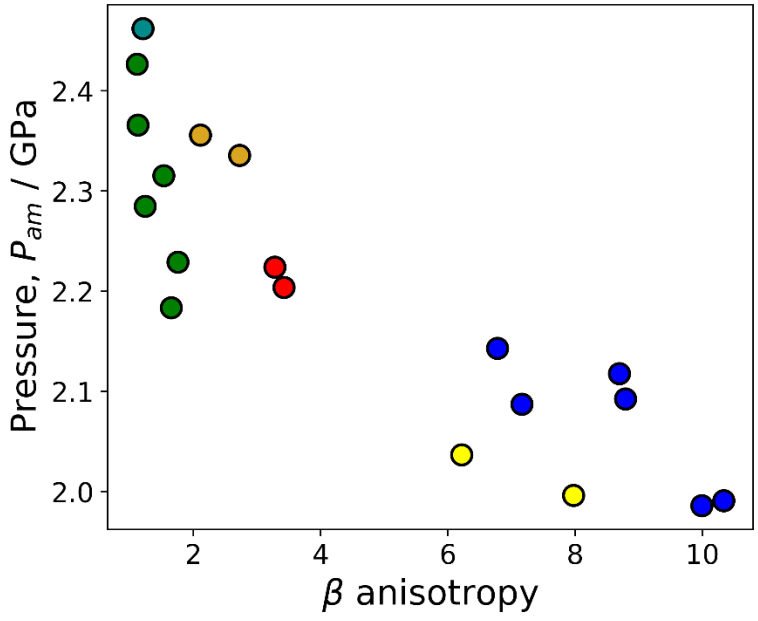

Figure S10: Amorphization pressure v.s anisotropy of linear compressibility modulus plot for the 19 structures containing 20 linker vacancies studied in this work. The data points are colored as indicated in Fig. S7

Results for structures with 4, 8, 12, 16 , 24, 28 and 32 vacancies

Structures with 4 defects											
Pam [GPa]	Dv [A]	Dc [A]	N Type1	N Type2	N Type3	N Type4	N Type5	N Type6	Kv [GPa]	Eani [GPa]	Bani [GPa]
2.792	18.12	12.59	0	1	0	1	1	1	57.80	1.18	1.10
2.797	19.28	16.67	0	2	0	0	2	0	57.76	1.22	1.22
2.802	22.31	15.69	0	0	1	0	2	1	57.73	1.19	1.14
2.802	10.12	7.32	1	1	1	1	0	0	58.00	1.17	1.09
2.817	20.92	25.05	0	0	2	0	0	2	57.92	1.22	1.21
2.817	16.79	11.34	1	0	0	1	1	1	57.91	1.18	1.11
2.817	10.83	19.16	2	0	1	1	0	0	58.38	1.18	1.11

Table S8: Comparison of amorphization pressure (Pam), mean distance between vacancies (Dv), mean distance to the center of the supercell (Dc), number of linkers according to orientation type, bulk modulus and anisotropies for the structures containing 4 defects studied in this work. Data is ordered according to amorphization pressure, in ascending order.

Structures with 8 defects											
Pam [GPa]	Dv [A]	Dc [A]	N Type1	N Type2	N Type3	N Type4	N Type5	N Type6	Kv [GPa]	Eani [GPa]	Bani [GPa]
2.533	26.54	18.92	0	0	0	8	0	0	55.53	1.54	1.739
2.665	22.07	22.57	8	0	0	0	0	0	55.38	1.561	1.7608
2.665	15.95	19.59	2	1	1	1	2	1	54.80	1.185	1.0923
2.670	22.75	21.39	0	0	8	0	0	0	55.20	1.614	1.8661
2.675	22.60	19.28	0	8	0	0	0	0	55.57	1.554	1.7465
2.685	22.48	17.71	2	4	0	2	0	0	55.34	1.234	1.2955
2.690	14.53	23.90	0	1	2	3	0	2	56.29	1.216	1.2055

Table S9: Comparison of amorphization pressure (Pam), mean distance between vacancies (Dv), mean distance to the center of the supercell (Dc), number of linkers according to orientation type, bulk modulus and anisotropies for the structures containing 8 defects studied in this work. Data is ordered according to amorphization pressure, in ascending order.

Structures with 12 defects											
Pam [GPa]	Dv [A]	Dc [A]	N Type1	N Type2	N Type3	N Type4	N Type5	N Type6	Kv [GPa]	Eani [GPa]	Bani [GPa]
2.482	19.46	21.39	3	2	2	3	1	1	51.74	1.20	1.19
2.498	21.52	19.55	0	12	0	0	0	0	53.40	1.99	2.61
2.558	21.54	18.46	12	0	0	0	0	0	53.84	1.85	2.27
2.579	20.48	20.11	1	2	4	2	1	2	51.97	1.23	1.28
2.599	20.79	19.24	1	3	2	2	2	2	52.59	1.22	1.21
2.599	19.54	21.44	1	3	2	2	0	4	52.47	1.30	1.33

Table S10: Comparison of amorphization pressure (Pam), mean distance between vacancies (Dv), mean distance to the center of the supercell (Dc), number of linkers according to orientation type, bulk modulus and anisotropies for the structures containing 12 defects studied in this work. Data is ordered according to amorphization pressure, in ascending order.

Structures with 16 defects											
Pam [GPa]	Dv [A]	Dc [A]	N Type1	N Type2	N Type3	N Type4	N Type5	N Type6	Kv [GPa]	Eani [GPa]	Bani [GPa]
2.092	23.05	19.89	0	0	0	16	0	0	50.71	3.02	7.21
2.204	23.51	19.89	0	8	0	8	0	0	49.59	1.73	2.65
2.219	21.95	19.89	0	0	8	8	0	0	48.34	1.36	2.17
2.239	24.08	18.92	0	0	8	8	0	0	51.47	1.50	2.02
2.300	17.60	23.75	2	4	1	3	3	3	46.73	1.26	1.19
2.310	22.48	19.89	8	0	0	8	0	0	50.92	1.62	2.08
2.361	18.46	21.87	2	2	0	3	5	4	48.36	1.36	1.52
2.381	15.45	11.34	4	1	2	4	2	3	49.26	1.27	1.39
2.412	24.08	19.89	0	0	8	8	0	0	52.05	1.43	1.62
2.427	24.08	19.89	0	0	0	0	8	8	52.05	1.43	1.62
2.442	20.22	22.30	2	1	4	2	2	5	48.92	1.27	1.33
2.447	23.05	18.92	0	0	0	16	0	0	53.65	1.85	2.22
2.457	23.05	18.92	0	0	0	0	0	16	53.65	1.85	2.22
2.503	21.08	21.27	1	1	2	4	3	5	50.45	1.26	1.26

Table S11: Comparison of amorphization pressure (Pam), mean distance between vacancies (Dv), mean distance to the center of the supercell (Dc), number of linkers according to orientation type, bulk modulus and anisotropies for the structures containing 16 defects studied in this work. Data is ordered according to amorphization pressure, in ascending order.

Structures with 24 defects											
Pam [GPa]	Dv [A]	Dc [A]	N Type1	N Type2	N Type3	N Type4	N Type5	N Type6	Kv [GPa]	Eani [GPa]	Bani [GPa]
1.996	21.94	20.22	16	0	8	0	0	0	46.17	3.11	7.32
2.027	22.39	18.92	8	8	0	8	0	0	46.50	1.68	2.48
2.072	18.37	18.76	7	1	4	6	2	4	43.67	1.55	1.92
2.108	16.23	11.82	3	5	4	5	3	4	42.80	1.21	1.29
2.118	18.90	22.79	5	4	2	7	3	3	44.73	1.30	1.48
2.118	19.68	23.06	4	5	4	5	3	3	42.39	1.25	1.27
2.168	21.00	19.99	3	1	6	5	7	2	43.72	1.41	1.68
2.194	21.93	19.57	0	8	8	8	0	0	48.23	1.56	1.85

Table S12: Comparison of amorphization pressure (Pam), mean distance between vacancies (Dv), mean distance to the center of the supercell (Dc), number of linkers according to orientation type, bulk modulus and anisotropies for the structures containing 24 defects studied in this work. Data is ordered according to amorphization pressure, in ascending order.

Structures with 28 defects											
Pam [GPa]	Dv [A]	Dc [A]	N Type1	N Type2	N Type3	N Type4	N Type5	N Type6	Kv [GPa]	Eani [GPa]	Bani [GPa]
1.783	20.55	19.14	0	0	0	14	0	14	44.12	2.72	8.28
1.869	19.11	24.75	6	5	5	8	1	3	41.69	1.67	1.80
1.880	20.87	20.43	14	0	0	0	14	0	44.79	2.60	6.33
1.895	19.83	20.89	3	5	9	1	1	9	41.67	1.84	2.97
2.001	19.24	17.06	6	4	5	4	4	5	39.28	1.38	1.56
2.032	20.98	19.88	0	0	0	0	14	14	45.91	2.37	6.11
2.077	18.65	15.79	4	4	7	5	4	4	40.99	1.20	1.19
2.153	20.18	21.36	3	3	7	6	3	6	42.91	1.24	1.37
2.168	20.26	20.50	3	5	5	5	5	5	41.99	1.28	1.16
2.204	20.63	20.01	6	4	3	5	6	4	42.67	1.26	1.28

Table S13: Comparison of amorphization pressure (Pam), mean distance between vacancies (Dv), mean distance to the center of the supercell (Dc), number of linkers according to orientation type, bulk modulus and anisotropies for the

structures containing 28 defects studied in this work. Data is ordered according to amorphization pressure, in ascending order.

Structures with 32 defects											
Pam [GPa]	Dv [A]	Dc [A]	N Type1	N Type2	N Type3	N Type4	N Type5	N Type6	Kv [GPa]	Eani [GPa]	Bani [GPa]
1.687	21.01	19.89	0	8	0	8	8	8	40.17	1.76	2.43
1.687	20.25	20.49	6	6	5	3	8	4	37.71	1.42	1.75
1.763	20.89	19.89	8	8	8	8	0	0	38.15	1.69	1.93
1.768	21.92	19.89	8	8	8	8	0	0	42.35	1.70	2.01
1.814	22.47	18.92	16	16	0	0	0	0	50.50	1.81	3.59
1.819	20.46	19.32	2	7	9	3	6	5	40.16	1.52	1.66
1.869	20.26	17.20	6	7	5	2	8	4	40.76	1.44	1.64
1.920	19.29	15.89	2	4	7	6	5	8	40.12	1.36	1.51
1.951	16.77	15.06	4	7	4	8	3	6	40.34	1.28	1.40
1.966	20.48	17.03	3	2	8	8	9	2	41.55	1.46	1.74
2.102	21.44	19.89	0	0	16	16	0	0	46.79	1.50	2.29

Table S14: Comparison of amorphization pressure (Pam), mean distance between vacancies (Dv), mean distance to the center of the supercell (Dc), number of linkers according to orientation type, bulk modulus and anisotropies for the structures containing 32 defects studied in this work. Data is ordered according to amorphization pressure, in ascending order.

Reference ordered												
N Vac	Pam [GPa]	Dv [A]	Dc [A]	N Type1	N Type2	N Type3	N Type4	N Type5	N Type6	Kv [GPa]	Eani [GPa]	Bani [GPa]
32	1.829	22.47	18.92	0	0	16	16	0	0	50.50	1.81	3.59
28	1.956	22.30	18.92	0	0	14	14	0	0	50.75	1.73	3.02
24	2.128	21.70	18.92	0	0	12	12	0	0	51.98	1.60	2.42
20	2.249	20.58	18.92	0	0	10	10	0	0	53.17	1.47	2.00
16	2.401	17.55	18.92	0	0	8	8	0	0	55.66	1.28	1.55
12	2.508	17.02	18.92	0	0	6	6	0	0	55.93	1.24	1.42
8	2.665	14.88	18.92	0	0	4	4	0	0	57.14	1.19	1.28
4	2.786	11.78	18.92	0	0	2	2	0	0	58.34	1.16	1.15

Table S15: Comparison of amorphization pressure (Pam), mean distance between vacancies (Dv), mean distance to the center of the supercell (Dc), number of linkers according to orientation type, bulk modulus and anisotropies for the reference set of 8 structures where the vacancies were introduced in an orderly fashion. Data is ordered according to amorphization pressure, in ascending order.

Reference random												
N Vac	Pam [GPa]	Dv [A]	Dc [A]	N Type1	N Type2	N Type3	N Type4	N Type5	N Type6	Kv [GPa]	Eani [GPa]	Bani [GPa]
32	1.829	22.47	18.92	0	0	16	16	0	0	50.50	1.81	3.59
28	1.981	22.44	19.57	0	0	15	13	0	0	50.71	1.75	3.01
24	2.143	22.32	19.89	0	0	12	12	0	0	51.21	1.57	2.33
20	2.275	22.26	20.08	0	0	8	12	0	0	52.07	1.55	2.15
16	2.391	22.29	19.95	0	0	7	9	0	0	52.87	1.40	1.76
12	2.503	22.42	19.33	0	0	6	6	0	0	53.93	1.29	1.53
8	2.670	22.39	18.08	0	0	3	5	0	0	55.81	1.22	1.35
4	2.797	19.55	14.35	0	0	1	3	0	0	58.21	1.19	1.19

Table S16: Comparison of amorphization pressure (Pam), mean distance between vacancies (Dv), mean distance to the center of the supercell (Dc), number of linkers according to orientation type, bulk modulus and anisotropies for the structures for the reference set of 8 structures where the vacancies were introduced in a random fashion. Data is ordered according to amorphization pressure, in ascending order.

References

[S1] Rappe, A.K., Casewit, C.J., Colwell, K.S., Goddard, W.A., III, Skiff, W.M., 1992. UFF, a full periodic table force field for molecular mechanics and molecular dynamics simulations. J. Am. Chem. Soc. https://doi.org/10.1021/ja00051a040

[S2] Boyd, P.G., Moosavi, S.M., Witman, M., Smit, B., 2017. Force-Field Prediction of Materials Properties in Metal-Organic Frameworks. J. Phys. Chem. Lett. https://doi.org/10.1021/acs.jpclett.6b02532. LAMMPS interface software page: https://github.com/peteboyd/lammps_interface

[S3] Dubbeldam, D., Calero, S., Ellis, D.E., Snurr, R.Q., 2015. RASPA: molecular simulation software for adsorption and diffusion in flexible nanoporous materials. Molecular Simulation. https://doi.org/10.1080/08927022.2015.1010082

[S4] Cavka, J.H., Jakobsen, S., Olsbye, U., Guillou, N., Lamberti, C., Bordiga, S., Lillerud, K.P., 2008. A New Zirconium Inorganic Building Brick Forming Metal Organic Frameworks with Exceptional Stability. J. Am. Chem. Soc. https://doi.org/10.1021/ja8057953